


RESEARCH ARTICLE

Investigation of the functional pathogenesis of mild cognitive impairment by localisation-based locus coeruleus resting-state fMRI

Thomas Liebe^{1,2,3,4} | Milos Dordevic⁵ | Jörn Kaufmann⁶ | Araks Avetisyan⁷ |
Martin Skalej⁸ | Notger Müller⁵ 

¹Department of Psychiatry, Medical University of Vienna, Vienna, Austria

²Department of Radiology, University Hospital Jena, Jena, Germany

³Department of Psychiatry, University Hospital Jena, Jena, Germany

⁴Clinical Affective Neuroimaging Laboratory, Leibniz Institute for Neurobiology, Magdeburg, Germany

⁵Department of Degenerative and Chronic Diseases, University Potsdam, Potsdam, Germany

⁶Department of Neurology, University Hospital Magdeburg, Magdeburg, Germany

⁷Neuroprotection Lab, German Center for Neurodegenerative Diseases (DZNE), Magdeburg, Germany

⁸Department of Neuroradiology, Clinic and Policlinic of Radiology, University Hospital Halle, Halle, Germany

Correspondence

Thomas Liebe, University Clinic for Psychiatry and Psychotherapy, Währinger Gürtel 18-20, 1090 Vienna, Austria.

Email: thomas.liebe@meduniwien.ac.at

Funding information

Deutsche Forschungsgemeinschaft, Grant/Award Number: 449879371

Abstract

Dementia as one of the most prevalent diseases urges for a better understanding of the central mechanisms responsible for clinical symptoms, and necessitates improvement of actual diagnostic capabilities. The brainstem nucleus locus coeruleus (LC) is a promising target for early diagnosis because of its early structural alterations and its relationship to the functional disturbances in the patients. In this study, we applied our improved method of localisation-based LC resting-state fMRI to investigate the differences in central sensory signal processing when comparing functional connectivity (fc) of a patient group with mild cognitive impairment (MCI, $n = 28$) and an age-matched healthy control group ($n = 29$). MCI and control participants could be differentiated in their Mini-Mental-State-Examination (MMSE) scores ($p < .001$) and LC intensity ratio ($p = .010$). In the fMRI, LC fc to anterior cingulate cortex (FDR $p < .001$) and left anterior insula (FDR $p = .012$) was elevated, and LC fc to right temporoparietal junction (rTPJ, FDR $p = .012$) and posterior cingulate cortex (PCC, FDR $p = .021$) was decreased in the patient group. Importantly, LC to rTPJ connectivity was also positively correlated to MMSE scores in MCI patients ($p = .017$). Furthermore, we found a hyperactivation of the left-insula salience network in the MCI patients. Our results and our proposed disease model shed new light on the functional pathogenesis of MCI by directing to attentional network disturbances, which could aid new therapeutic strategies and provide a marker for diagnosis and prediction of disease progression.

KEYWORDS

attention, locus coeruleus, mild cognitive impairment, resting-state fMRI

Abbreviations: ACC, anterior cingulate cortex; AD, Alzheimer disease; BOLD, blood-oxygen-dependent; DMN, the default mode network; EPI, echo-planar imaging; FDR, false discovery rate; FOV, fields of view; LC, locus coeruleus; LOC, lateral occipital cortex; MCI, mild cognitive impairment; MMSE, mini-mental state examination; MRI, magnetic resonance imaging; PCC, posterior cingulate cortex; ROI, region of interest; rs-fMRI, resting-state functional MRI; TE, echo time; TI, inversion time; TPJ, temporoparietal junction; TR, repetition time.

This is an open access article under the terms of the [Creative Commons Attribution-NonCommercial-NoDerivs](https://creativecommons.org/licenses/by-nc-nd/4.0/) License, which permits use and distribution in any medium, provided the original work is properly cited, the use is non-commercial and no modifications or adaptations are made.

© 2022 The Authors. *Human Brain Mapping* published by Wiley Periodicals LLC.

1 | INTRODUCTION

Dementia is one of the most prevalent and compelling diseases arising in the 21st century (Cao et al., 2020; Prince et al., 2013) with an expected number of 135 million patients worldwide in 2050 (Robinson et al., 2015). There is urgent need for an improvement of understanding of the underlying mechanisms in the brain responsible for clinical symptoms, and improvement and extension of diagnostic capabilities (Lorking et al., 2021; McCarthy et al., 2018; Tsoi et al., 2015). Especially, an early diagnosis is crucial for a timely intervention aiming at preventing disease progression and at alleviating of symptom severity (Barnett et al., 2014; Crous-Bou et al., 2017; Robinson et al., 2015). In this respect, the small bilateral brainstem nucleus locus coeruleus (LC) gains increasingly attention because of both its functionality related to dementia symptoms and its known early structural alterations in dementia (Betts et al., 2019; German et al., 1992; Samuels & Szabadi, 2008; Tomlinson et al., 1981). The disturbances in LC structure appear in line with early clinical symptoms and long before classical structural alterations like volume loss of temporal lobes can be detected in magnetic resonance imaging (MRI; Olivieri et al., 2019; Takahashi et al., 2015). Both mild cognitive impairment (MCI) and Alzheimer disease (AD) studies could show an increase of plaques accumulating within the LC, and the relationship of those molecular changes was correlated to the early symptoms and the progression of the disease (Elman et al., 2021; Markesbery, 2010; Tomlinson et al., 1981). Furthermore, the signal intensity of the LC as seen in specialised MRI sequences correlates to the LC noradrenaline cell count (Keren et al., 2015), and was found to be directly aligned to disease severity (Betts et al., 2019; Clewett et al., 2016; Dordevic et al., 2017; Liu et al., 2020).

Beyond assessing structural alterations, functional methods can provide insight into the disturbances in brain networks related to dementia, improve the understanding of the impact of the structural changes within and between the affected brain areas, and may support the early diagnosis of the disease even before structural disturbances become evident. One important capacity of human behaviour that is heavily affected in MCI patients is human attention: Dementia patients are characterised by difficulties in activities of daily living such as spatial orientation, concentration, and planning, especially in the early stages of dementia, which may often have been overlooked (Bradford et al., 2009; Coughlan et al., 2018; Sanders et al., 2014; Saunders & Summers, 2011). Those symptoms underlie impairments in visuospatial attention, sustained attention, and executive functioning, respectively—which constitute the major facets of attention network functions (Baddeley et al., 1999; Berardi et al., 2005; Brandt et al., 2009; Costa et al., 2020; Faust & Balota, 1997; Redel et al., 2012; Waninger et al., 2018).

The LC is directly related to the clinical alteration and networks found here: It is involved in sustained attention and vigilance, and further in the selection of relevant sensory signals within the alerting, frontal and dorsal attention networks (Aston-Jones & Cohen, 2005a; Corbetta et al., 2008; Périn et al., 2010). Beyond and bound to the LC, the salience network is widely described as the relevant entity to transfer information of the relevance of sensory signals to the frontal

brain to guide decision processes (Aston-Jones & Cohen, 2005b; Seeley, 2019). Within the salience network, the insula receives information about the quality of internal and external world signals and transfers those signals to the anterior cingulate cortex (ACC). The ACC as the frontal-brain hub for decision making, then controls the LC in its electrophysiological behaviour in respect to the behavioural relevance of those signals (Aston-Jones & Cohen, 2005b). The LC—in dependence of the ACC control—can then enhance sensory signals in all the brain by promoting noradrenaline spillover to a wide range of target cells, and selectively enhance memory, reaction, and consciousness (Berridge & Foote, 1991; Berridge & Waterhouse, 2003).

Still, there are limitations in investigating those functional relationships between brain regions—especially, the LC is a very small nucleus and could benefit from improved methods when measuring functional MRI (fMRI). In our previous work, we advanced the measurement of the LC functional connectivity (fc) signal by previous delineation of the nucleus based on its neuromelanin contrast and extraction of the blood-oxygen-dependent (BOLD) signal at the exact intraindividual position of the nucleus in the brainstem (Liebe et al., 2020).

In the following study, we investigated the rs-fc of the LC comparing a group of MCI patients and a group of age-matched healthy control participants. For measurement of the BOLD signal, we applied our improved method of LC fc measurement. We expected disturbances in the LC network and salience network in the MCI patients, and predicted, that those networks would be related to behavioural measures of the mini-mental state examination (MMSE), which is the score that is most widely validated and assessed in dementia patients (Arevalo-Rodriguez et al., 2015), and broadly investigated in conjunction with fMRI studies (Balthazar et al., 2014; Cha et al., 2013; Liao et al., 2018; Yokoi et al., 2018; Zheng et al., 2019).

We aim to advance the understanding of how brain networks are affected in MCI and to show a practical use case for the application of improved methods in terms of LC fc.

2 | MATERIALS AND METHODS

2.1 | Study design and ethical approval

This study was designed as cross-sectional with one factor: group (control, MCI). All measurements took place from February 2019 to March 2020 in Magdeburg at two sites—namely, the German Center for Neurodegenerative Diseases and the Department of Neurology of the Otto von Guericke University Clinic. Ethical approval (165/18) was obtained from the ethics committee of the Otto von Guericke University—Medical Faculty, Magdeburg, Germany.

2.2 | Participants

Patients aged between 50 and 85 years were recruited between February 2019 and March 2020 from the memory clinic at the Department of Neurology of the Otto von Guericke University Clinic,

Magdeburg, Germany (Figure S2). The diagnosis of MCI had been established by an experienced neurologist of the memory clinic according to the NINCDS-ADRDA criteria (McKhann et al., 1984). Their MMSE scores were at minimum 20 or higher. Patients were excluded from the study if they had any systemic neurological, orthopaedic, cardiologic, or metabolic disease, tattoo or metal-based implants in the body, a brain operation which would affect MRI analysis, or uncorrected reduced visual ability. In total, 28 patients were tested and were age- and gender-matched with healthy participants of the control group; there was no significant difference in age between the patient ($n = 28$, 73.3 ± 7.5 years [range 51–85], 14 females) and control ($n = 29$, 71.8 ± 8.1 years [range 50–85], 15 females) groups ($p = .496$). The participants of the healthy control group had an MMSE score of 27 or higher.

2.3 | Neuropsychological tests (CERAD-Plus)

The applied version of CERAD-Plus test-battery includes 11 subtests: Verbal Fluency (animals in 60 s), 15-item Boston Naming Test, MMSE, Word List Learning, Word List Recall, Word List Recognition, Constructional Praxis, Delayed Constructional Praxis, Clock Drawing, Trail-Making Tests A and B and Phonemic Fluency (S-words in 60s). In this study, the MMSE was used to assess the relationship between rs-fc and behavioural score, since the MMSE is the most widely used screening tool, has a high acceptance as a diagnostic instrument and provides an overall view about patients' abilities (Arevalo-Rodriguez et al., 2015). All patients were tested with the CERAD-Plus. In the healthy control group, with 22 from 29 participants, the CERAD-Plus test battery could be performed. MMSE results were compared between MCI and control groups with a *t*-test of independent samples.

2.4 | MRI data acquisition

MR images were acquired on a high-field 3 T Skyra MR tomograph with a 32-channel head array coil (Siemens Healthineers, Erlangen, Germany). Every subject underwent structural MRI, resting-state fMRI (rs-fMRI) and neuromelanin-sensitive Turbo spin echo (TSE) sequence acquisition in the same session.

The high-resolution T1-weighted anatomical MR image was acquired, using a magnetisation-prepared rapid gradient-echo sequence with the parameters as follows: echo time (TE) = 4.32 ms, repetition time (TR) = 2500 ms, inversion time (TI) = 1100 ms, flip angle = 7, fields of view (FOV) = 256 mm, 192 sagittal slices, acc. Factor: grappa 2, bandwidth = 140 Hz/pixel, and isotropic voxel size = 1 mm.

For the eyes-closed rs-fMRI scans a T2*-weighted echo-planar imaging (EPI) sequence was applied with the following parameters: TE = 30 ms, TR = 2.0 s, FOV = 220 mm, 66 axial slices parallel to the anterior-posterior commissure plane covering the whole brain acquired in interleaved order, slice thickness = 2.20 mm, isotropic

voxel size = 2.20 mm, multiband acceleration factor = 2, acceleration factor = grappa 2, flip angle = 80, 320 volumes in total, and scan duration = 11 min.

Since geometric distortions are caused by magnetic field inhomogeneities in EPI sequences, a field map was acquired using a double-echo gradient recalled echo sequence (TE 1/2 = 4.92 ms/7.38 ms, TR = 660 ms, flip angle = 60, isometric voxels size of 2.2 mm, FOV = 220 × 220 mm², 66 slices aligned with the fMRI slices, and scan duration = 2 min 13 s).

Neuromelanin serves as an endogenous MR contrast agent: by shortening the longitudinal relaxation time T1, the LC becomes visible hyperintense in high-resolution T1-weighted MRI. Thus, we acquired a neuromelanin sensitive TSE sequence, according to the original publication 41 with the following parameters: 14 axial slices, acquisition volume = 192 × 192 × 42 mm³, slice thickness = 2.50 mm, inter-slice gap 0.5 mm, leading to an effective slice thickness of 3 mm, TR = 634.0 ms, TE = 10.0 ms, bandwidth = 165 Hz/Pixel, flip angle = 180, and scan duration = 10 min 50s.

2.5 | MRI data pre-processing

We pre-processed our data in accordance with our previous publication (Liebe et al., 2020), as we compared pipelines with extraction of the LC signal in both subject and Montreal Neurological Institute (MNI) space. In this study, we focussed on our advanced method of extracting the BOLD signal from the individual LC location in every subject and only exploratory investigated LC fc based on the MNI space approach.

LC masks for fMRI signal extraction were drawn by a radiologist experienced in neuroradiology in FSLview (<https://fsl.fmrib.ox.ac.uk/fsl/>) based on the neuromelanin contrast of the nucleus. For registration, binarisation, and interpolation of the mask, FSL FLIRT and fslmaths (<https://fsl.fmrib.ox.ac.uk/fsl/>) were used. For details of our method, we refer to our previous publication (Liebe et al., 2020).

The sizes of the masks were compared using fslstats (<https://fsl.fmrib.ox.ac.uk/fsl/>), revealing no difference in the size between groups (at 1 mm isotropic voxel size resolution: Controls mean = 143.6 voxels, SD = 14.60; MCI mean = 140.4, SD = 19.00; two-sample *t*-test $p = .475$). In line with our previous publication (Liebe et al., 2020), the masks were in the mean smaller than a commonly used MNI space mask (216 voxels, Keren et al. 2SD mask; Keren et al., 2009), reflecting the improvement in individual localisation of the nucleus compared with using a mean MNI space group mask based on a representative population.

Detailed processing of LC intensity was published in our previous work (Dordevic et al., 2017). In brief, before image analysis, all scans were sinc-interpolated with a rectangular window of 11 voxels to the in-plane resolution of 0.25 mm using FSL flirt. For quantitative evaluation of the high-resolution TSE T1-weighted image, signal intensities were measured using the FSL software library (<https://fsl.fmrib.ox.ac.uk/fsl/fslwiki/>; Oxford, UK). In fslview, masks were created in two subsequent tomographic slices (each 2.5-mm thick) starting with the slice

7.5 mm below the level of the substantia nigra-pars compacta and the inferior colliculus (Figure S1). Within both slices, four masks were manually created: (1) left LC, (2) right LC, (3) left pontine reference region, and (4) right pontine reference region. Using functions `fslmaths` and `fslstats`, the maximum intensity values were extracted from each of the masks created. Finally, ratios were determined within each slice by dividing the maximum value of the left LC with its respective left pontine reference region and for the right LC with the respective right pontine reference region. In this way, we obtained two intensity ratios for each slice, one for each side; given that we measured two subsequent slices, we acquired a total of four values for the intensity ratios per subject. A total of three subjects had to be excluded from this analysis because of bad image quality due to motion artefacts. LC intensity values were compared between groups with a *t*-test of independent samples. The significance threshold was set to a $p = .0125$ by Bonferroni correction to the number of four slices.

For the pre-processing of the fMRI data, the standard CONN pre-processing pipeline, which is based on the SPM12 toolbox (<https://www.fil.ion.ucl.ac.uk/spm/>; Whitfield-Gabrieli & Nieto-Castanon, 2012), was used with some modifications. The pre-processing steps included simultaneous realignment, unwarp, and field map correction of functional data, slice time correction (with slice timings provided to SPM, as we used a multiband sequence), ART-based outlier detection (conservative settings), and direct functional-to-anatomical registration for every subject. We denoised the data by regression of white matter and CSF signals, removal of linear/quadratic trends, regression of subject motion (three-rotation and three-translation parameters as well as their first-order temporal derivatives), removal of motion outliers (scrubbing) and band-pass filtering at 0.008–0.09 Hz. In comparison to our previous publication, we further advanced the definition of white and grey matter anatomy for the denoising step by applying the FreeSurfer segmentation algorithm (<http://surfer.nmr.mgh.harvard.edu/>, as suggested by Reuter et al., 2012) and importing the segmentation maps of grey and white matter into CONN. The mean BOLD signal was then extracted from the unsmoothed EPI data in the individual anatomical image subject space within the individual LC masks created as formerly described. This process was followed by structural and functional direct normalisation of the EPI images to MNI space (structural target resolution 1 mm, functional target resolution 2 mm) and smoothing with a 4 mm kernel. The extracted subject-specific, individual LC time courses were then voxel-wise correlated to the individual whole-brain MNI space functional data. The target regions of interest (ROIs) were defined by the default atlas implemented in CONN which covers the whole brain (comprising the FSL Harvard-Oxford Atlas; <https://fsl.fmrib.ox.ac.uk/fsl/fslwiki/>) and cerebellar parcellation from automated anatomical atlas (AAL) (Tzourio-Mazoyer et al., 2002). Second, we extracted the LC signal from the individual unsmoothed, MNI space registered functional volumes with a widely validated MNI space mask (Keren et al., 2009, 2015) to show the superiority of the subject-specific approach, as previously reported (Liebe et al., 2020).

To be able to sub-specify connectivity results of our main pipeline in a secondary analysis, we additionally sub-segmented the brain based on the parcellation of Glasser et al. (2016) to gain insights into functionally relevant subregions: We processed the T1 images using the FreeSurfer pipeline (Fischl, 2012) version 7.0 with default parameters, with ROIs defined according to the HCP MMP 1.0 atlas (Glasser et al., 2016). The output of every subject was checked visually by viewing the subcortical segmentation and the white and pial surfaces using the `freeview` FreeSurfer tool. The resulting segmentations (`aparc-` and `aseg-`files) comprised all cortical and subcortical regions (180 atlas regions on each cortical hemisphere, plus 19 subcortical regions [2×9 plus brainstem]), which resulted in a total of 379 nodes as target ROIs. By using the MRtrix (Tournier et al., 2019) tools `mrcalc` and `mrtransform`, the individual segmented LC region masks were integrated into the parcellation image. The parcellation image was then used to extract timecourses of the individual segmented LC brain regions and individual segmented target ROIs within the same CONN pre-processing pipeline as delineated above from the unsmoothed EPI data within the individual anatomical image subject space.

2.6 | fMRI—statistical analysis

Equations for our calculation of seed-to-voxel analysis within CONN (Whitfield-Gabrieli & Nieto-Castanon, 2012) are reported in the Supplementary Material of our previous publication (Liebe et al., 2020). For all analyses, the cluster defining threshold was set to a threshold of $p < .001$ at voxel level. Only clusters below a threshold of a False Discovery Rate corrected (FDR) $p < .05$ were reported to be significant in the seed-to-voxel analysis.

Whole sample LC connectivity was reported after conducting a one-sample *t*-test. We additionally investigated the whole sample LC connectivity with a *F*-test combining the separate effects of MCI and control groups (contrast [1 1]) to visualise the differences in LC group connectivity (any-effects analysis).

Since changes in left parahippocampal connectivity of LC were previously highlighted in MCI patients (Engels et al., 2020; Jacobs et al., 2015), we extracted the beta-values of the two clusters in the left parahippocampal gyrus, which were significantly connected to the LC in the whole sample assessment, and compared the group effects with a two-sample *t*-test in SPSS. Since two clusters were investigated, we adjusted the result according to the Bonferroni correction.

This hypothesis-driven assessment was followed by a one-way Analysis of Covariance (ANCOVA) covariate control analysis contrasting seed-based anatomical LC *fc* of MCI and control groups at whole brain level, while controlling for LC intensity values (slice *r*₁, which differed MCI and Control groups).

Subnuclei ROI-to-ROI analysis was applied on a constrained subset of regions (left frontal opercular [FOP]2, FOP3, FOP4, FOP5, AAI, ACI, AI, POI1, POI2, and Ig; for definition see Glasser et al., 2016) representing the left insula region that was found significant in the main test to sub-specify the result. LC to left insula subnuclei connectivity was FDR $p < .05$ corrected on seed-level with a one-sided

(positive) test (two-sample *t*-test with factor group), after permutation testing was performed (1000 iterations). Within-left insula connectivity was investigated FDR $p < .05$ corrected on analysis-level with a two-sided test (two-sample *t*-test with factor group), to account for multiple testing of all subnuclei without previous hypothesis, after permutation testing was performed (1000 iterations).

Left-insula salience network connectivity (based on the CONN predefined left insular salience network mask, see Table S2) was then investigated with a two-sample *t*-test on whole-brain level comparing MCI and control groups.

To compare regressions of MMSE scores between groups on a whole brain seed-to-voxel basis, one-way ANCOVA covariate interaction was assessed for LC and salience network seed-based connectivity (first factor LC or salience network fc of MCI and Control groups, second factor MMSE scores of MCI against Control groups).

Since MMSE scores were positively correlated to LC–right lateral occipital cortex (LOC) connectivity investigating the whole sample on whole-brain level, beta-values of significant change of LC–

right LOC difference between MCI and control groups were extracted, outliers removed (2 SD above or below the mean), and Pearson correlated to MMSE scores (positive directed one-side test, Figure 3c). In the bar graphs of Figures 2, 3 and 4, *h* values were reported as a measure of effect size. The *h* values represent the mean Fischer transformed pairwise correlations between the source region (LC or left insula salience network seed) and the significant whole-brain voxel clusters.

3 | RESULTS

3.1 | Behavioural results

The MMSE scores significantly differed between MCI and Control groups, as expected with lower scores of the MCI patients in the MMSE (MCI mean = 25.79, SD = 2.409; Control mean = 28.91, SD = 1.019; $p < .001$, Figure 1a).

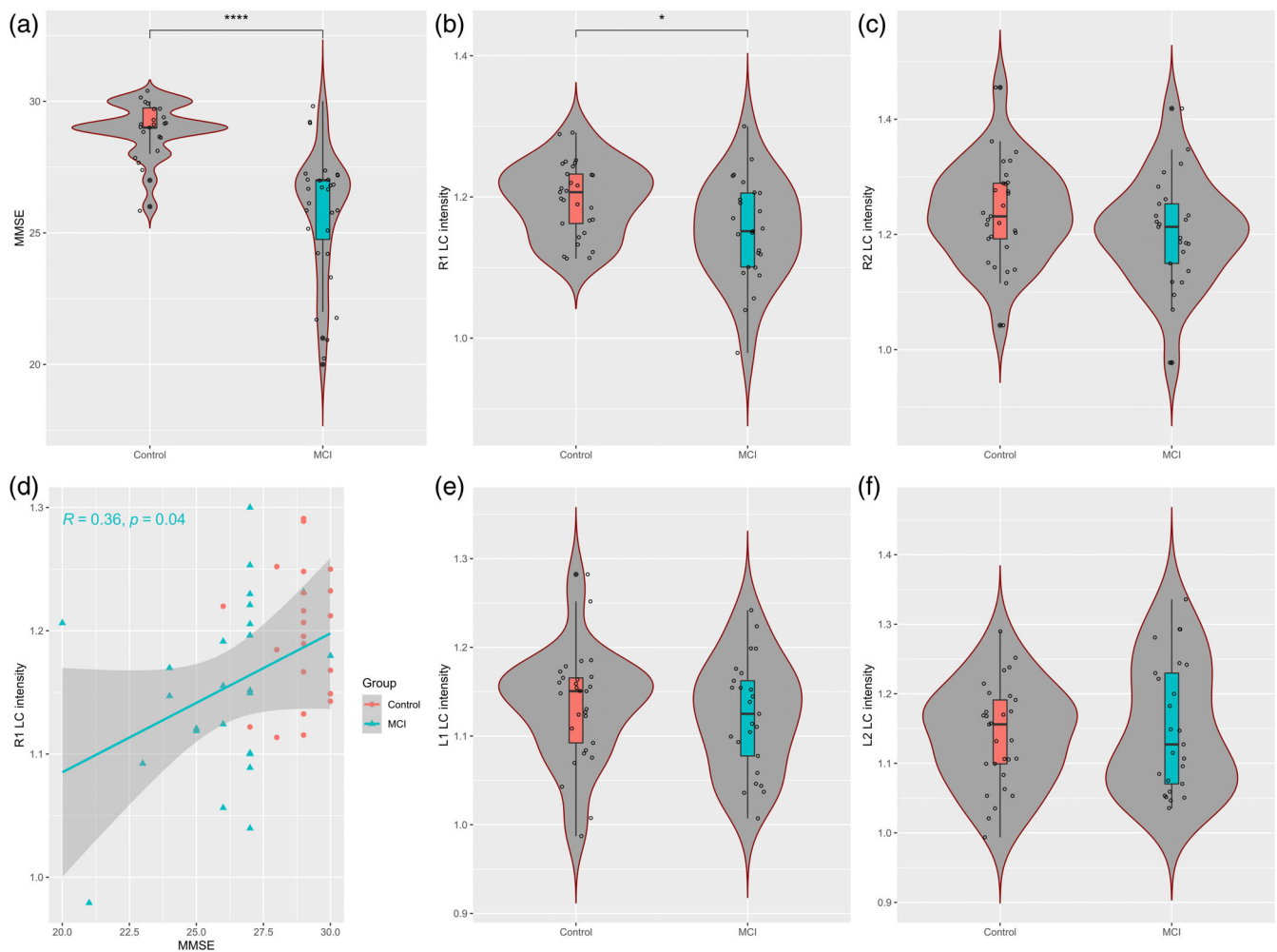


FIGURE 1 (a) Behavioural data and LC intensity results. MCI and control groups significantly differed in the mini-mental state examination (MMSE) scores. (b,c,e,f) In the four positions of locus coeruleus (LC) neuromelanin signal extraction, MCI patients showed lower intensity ratios in region r1 (b) compared with healthy control participants ($p = .010$). (d) We found a significant correlation between the signal intensity of r1 and MMSE scores (MCI group $p = .040$)

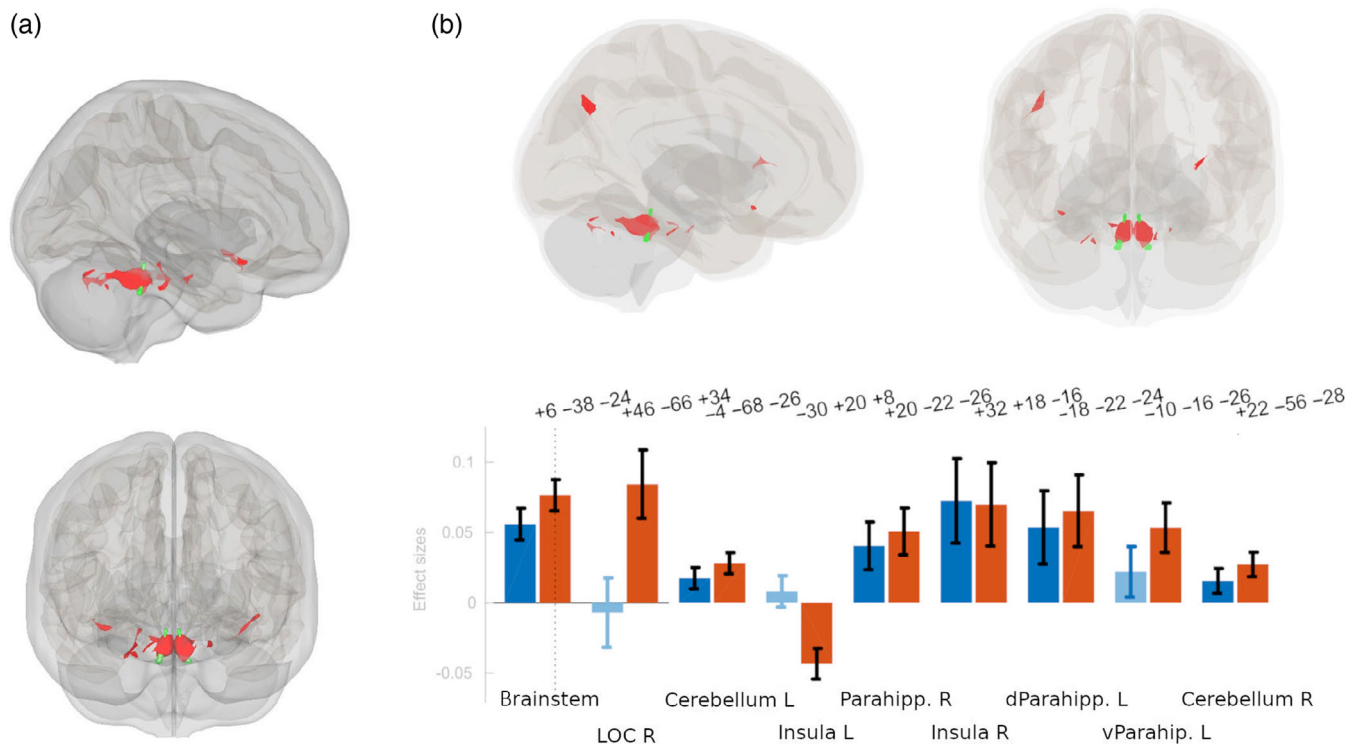


FIGURE 2 Baseline findings of localisation-based LC functional connectivity to the whole brain. (a) The whole brain analysis over all participants reveals strong LC (green) connectivity to brainstem, cerebellum, parahippocampal gyrus and insula bilaterally (red). (b) An any-effects analysis reveals differences of LC connectivity in the mild-cognitive impairment (MCI, blue) group compared with age-matched control group (red) in respect to the left insula, left ventral parahippocampal gyrus and right lateral occipital cortex (LOC)

3.2 | LC intensity results

In one of the four extracted positions of LC signal intensity, the ratio differed between age-matched control and MCI groups, and was found significant when controlling for all slices investigated (slice r1; MCI mean = 1.15, SD = 0.07; Control mean = 1.20, SD = 0.05; $p = .010$, Figure 1b). Furthermore, there was a significant positive correlation between the signal intensity of this slice and the MMSE scores of the MCI group ($r = 0.357$, $p = .04$, Figure 1d).

3.3 | fMRI LC connectivity

First, we averaged the results of all participants to investigate the overall LC fc as a whole. The LC was connected with the surrounding brainstem, the cerebellum, the parahippocampal gyrus bilaterally and with left and right insula (Figure 2a). An any-effect analysis revealed the same effects, but additionally showed the relevance of the right LOC in the general LC connectivity within the two groups (Figure 2b). Furthermore, the comparison of LC connectivity to the respective regions with significant LC interaction showed the general tendency of the MCI group to exhibit difference in LC fc to the LOC and the insular cortex (Figure 2b).

3.4 | fMRI LC connectivity group differences

Comparing the MCI and control group LC fc on the whole brain level, we found increased fc from the LC to the left insula (FDR $p = .012$) and ACC/paracingulate cortex (FDR $p < .001$), and reduced fc from the LC to the right LOC (FDR $p = .012$) and to the dorsal posterior cingulate cortex (PCC; FDR $p = .021$; Figure 3a,b).

Based on the previous findings from Jakobs et al. (Engels et al., 2020; Jakobs et al., 2015), we additionally focussed on the LC-left parahippocampal connectivity, and could find a reduced connectivity of the LC to the left ventral parahippocampal gyrus in the MCI patients ($p = .042$).

3.5 | ROI-to-ROI subnuclei analysis

To further specify our main finding of LC-insula connectivity changes, we analysed the connectivity of the LC signal in an ROI-to-ROI analysis to the Glasser-parcelled left insula. LC connectivity decrease was found in the left anterior ventral insular (FDR $p = .03$), and within the insula a connectivity decrease was found between left anterior agranular insula and left FOP5 (FDR $p = .006$).

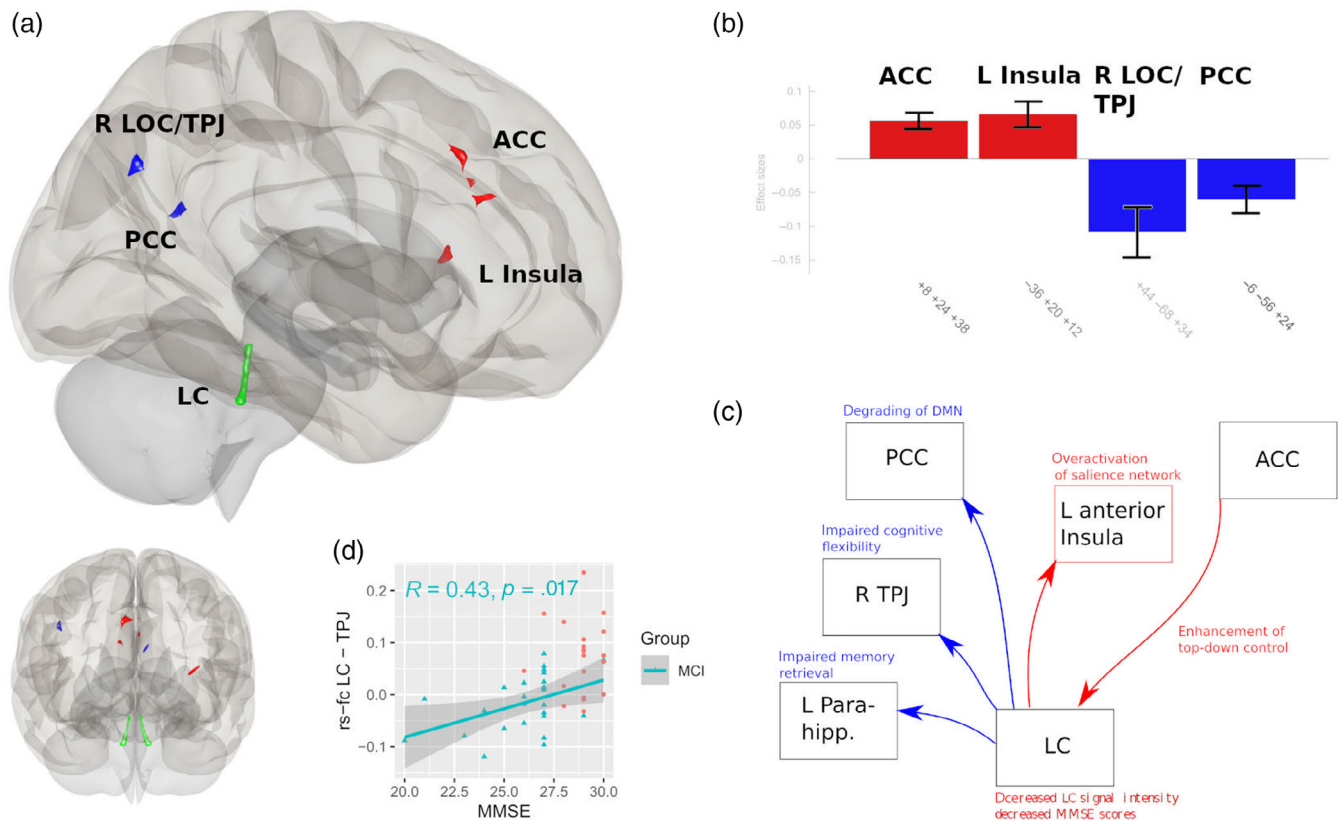


FIGURE 3 Differences of locus coeruleus (LC, green) resting-state functional connectivity (rs-fc) between mild-cognitive impairment (MCI) and age matched control group. (a,b) the LC rs-fc of the MCI patients was higher (red) to the ACC (FDR $p < .001$) and left insula (FDR $p = .012$), and lower (blue) to the posterior cingulate cortex (PCC, FDR $p = .021$) and right lateral occipital cortex (LOC, FDR $p = .012$). (c) Significant correlation of LC-temporoparietal junction (TPJ) connectivity and MMSE scores in the MCI group ($p = .017$). (d) Proposed model of impaired information processing in MCI patients based on the results of this study

3.6 | Relationship of LC fc to MMSE scores

LC fc to right LOC was positively correlated to MMSE scores in the MCI patients on whole brain level (FDR $p = .003$), which means that patients with higher LC LOC connectivity could better preserve their behavioural scores. We also extracted the beta-values of the LC fc to the LOC ROI shown to differ in the LC fc between MCI and control groups (Figure 3a,b) and could demonstrate a significant positive correlation to the MMSE scores in MCI patients ($p = .017$; Figure 3c for correlation of extracted beta-values of MCI patients to LC LOC fc).

3.7 | Salience network group differences

Since we found the left insula involved in the fc differences and based on previous research, we investigated the fc differences between MCI and control group regarding the left insula–salience network. The MCI and control groups differed in their fc to the bilateral cerebellum (right cerebellum FDR $p = .025$, left cerebellum FDR $p = .049$) and the left frontal pole (FDR $p = .028$; Figure 4b).

3.8 | fMRI LC and salience network group differences in respect to the MMSE

For the whole sample MMSE correlation to LC fc, we found significant clusters in the right LOC (FDR $p < .001$), the frontal pole left (FDR $p = .013$) and right precuneus (FDR $p = .036$). Comparing the MCI and control groups in terms of their relationship to the MMSE, we found more negative fc to the LC to the left frontal pole (FDR $p = .007$), middle/superior temporal gyrus (FDR $p = .007$) and the left hippocampus and parahippocampal gyrus (FDR $p = .013$) in the MCI patients in correlation to higher MMSE scores (Figure 4a). The relation of MMSE and left-insula salience network connectivity differed to big clusters of the frontal brain involving the frontal pole bilaterally, the superior frontal gyrus bilaterally and the paracingulate gyrus bilaterally (all FDR $p < .001$), the left middle and inferior temporal gyrus (FDR $p < .001$; Figure 4c). Post hoc tests revealed that those effects were driven by strong negative correlation of left and right frontal pole left-insular connectivity to MMSE in the MCI group (FDR $p < .001$); whereas in the control group strong positive correlations were found to the superior frontal gyrus and paracingulate gyrus, which were not found in the MCI group.

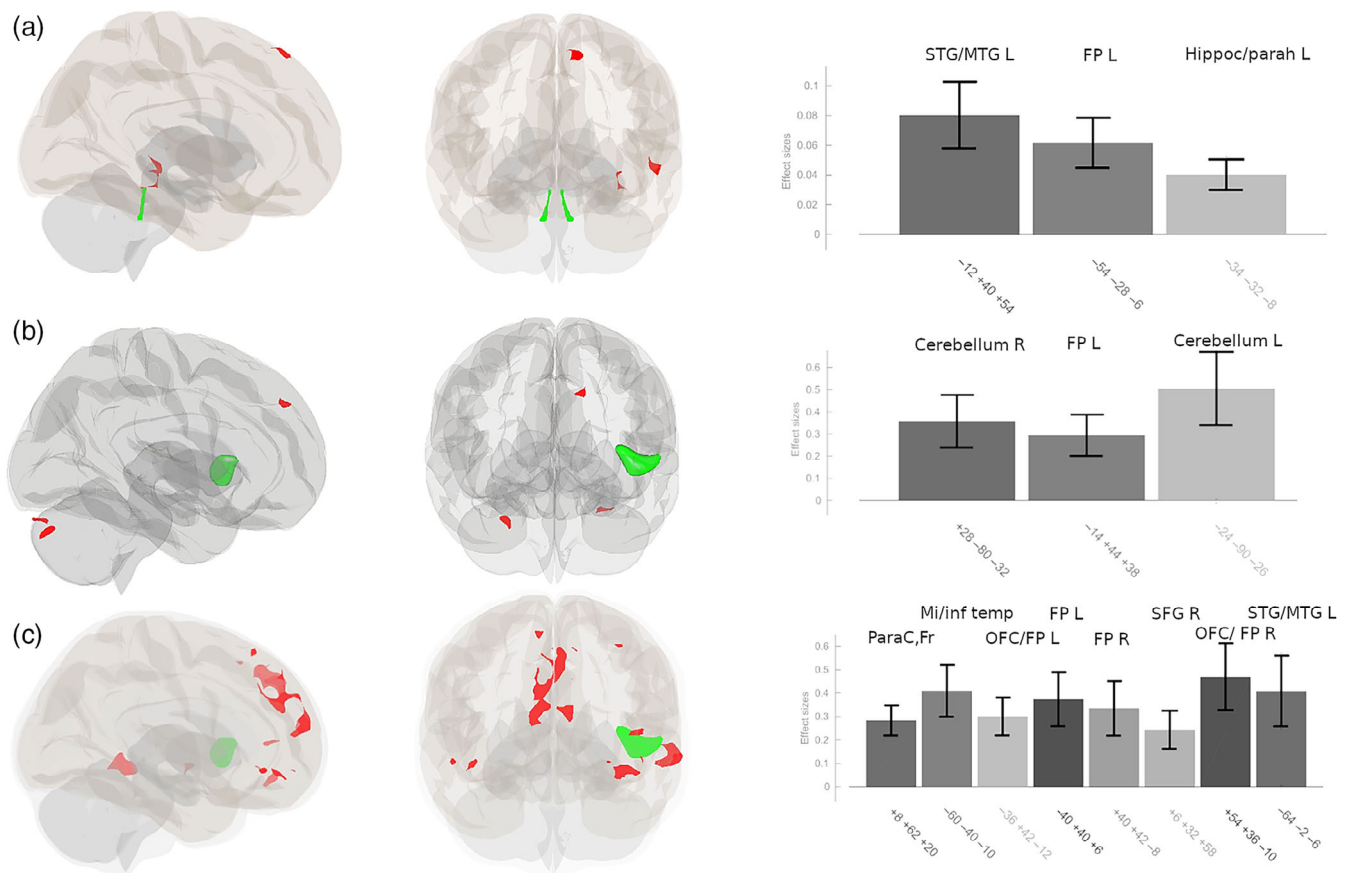


FIGURE 4 (a) Difference of relationship of the mini-mental state examination (MMSE) between MCI and control group in locus coeruleus (LC, green) functional connectivity (fc), where the hippocampal region, the frontal pole and the left temporal cortex differ in their correlation to the score. (b) Group differences of insula-salience network fc (green) reveals overactivation/increased connectivity to the frontal brain and bilateral cerebellum in MCI patients. (c) Correlation differences within anterior insula left-salience network (green) fc between MCI and control groups were found to frontal brain and left temporal regions

3.9 | MNI space LC mask

Additionally, to replicate our former results of superiority of subject-masked based LC signal extraction (Liebe et al., 2020), we extracted the LC signal out of the MNI space mask only. The whole sample results were similar, but the approach—as previously investigated—was not sensitive enough to reveal group differences between MCI and control participants as reported here.

4 | DISCUSSION

By advancing the measurement of LC fc by extracting the signal from the exact intraindividual location of the nucleus, we could uncover the involvement of LC and its link to the concomitant salience network in the functional pathogenesis of MCI. Furthermore, we show how both of these networks are related to a widely used behavioural score of dementia, to underpin their relevance for a concept of LC and salience network-related attentional changes in early dementia.

First, comparing our patient and healthy control study population showed a clear impairment of the MMSE values and of LC signal

intensity in the MCI group (in line with Dordevic et al., 2017; Figure 1a,b). Importantly, a direct relationship of this structural alteration of the LC and the behavioural score was found with high LC signal intensity maintaining adequate behaviour (Figure 1d).

In respect to our primary research question of functional disturbances in MCI patients, we then mapped the whole sample fc of the LC and found our results compatible with previous studies revealing LC connectivity (Jacobs et al., 2018; Liebe et al., 2018; 2020; Murphy et al., 2014; Wagner et al., 2018; Zhang et al., 2016) to the cerebellum, the brainstem, the parahippocampal gyrus and the insula.

An analysis of group differences between MCI and healthy controls revealed that ACC to LC connectivity is elevated in MCI patients. As pointed out in our former methodological study (Liebe et al., 2020), LC ACC connectivity could be a marker of how the frontal brain controls LC activity within the executive control network from “top-down” (Aston-Jones & Cohen, 2005b; Petersen & Posner, 2012; Posner, 2012). This process could initiate concomitant changes in attentional processing networks we also found: The connectivity between LC and the anterior insula, which is the seed region of the salience network, was heightened in our MCI patient group. In principle, the interaction between LC and the salience network is expected

to decline with ageing (Lee et al., 2020). In line with this view, especially the connectivity of LC to the left insula was found to be very low in our elderly control group, even in the negative, disconnected range. In our MCI disease study population, we however revealed a marked increase in the connectivity from LC to the left anterior insula (Figure 3).

Following this result and based on the hypothesis of attention network disturbances in the early stages of dementia, we found a hyperactivation of the left anterior insula salience network. The anterior insula forms an input hub of salience by receiving information of internal (body sensations) and external (outer) world (Farb et al., 2013; Mesulam & Mufson, 1982; Wang, Wu, et al., 2019; Witzel et al., 2018). In this process, the insula is responsible for weighting those inputs by interoceptive predictive coding and, in the last instance, integrate them into our subjective sense of reality and of the view of the self within the world (Seth, 2013; Seth et al., 2012). Consequently, insula pathology in dementia was discussed in terms of the loss of sense of self (Bonthius et al., 2005), apathy (Moon et al., 2014), self-concept (Philippi et al., 2020), and insula activity even seems to be protective in AD (Lin et al., 2016). Importantly, several other studies also found the insular network to be altered in dementia (Lu et al., 2020; Wang et al., 2021; Xie et al., 2012). Furthermore, studies revealed a phase of hyper- before a phase of hypoconnectivity within the salience network in respect to TAU and amyloid deposition in the brain (Schultz et al., 2017). The hyperconnectivity found here in the early stage of MCI as in our patient population suggests a compensatory mechanism of a hyperactive salience processing, that may be necessary to maintain behavioural performance (Zhou et al., 2010).

We then found a decline in fc from the LC to the PCC. The PCC is the posterior hub of the default mode network (DMN) and has modulatory influence on the network (Wang, Chang, et al., 2019). The alteration of LC to PCC may suggest a degrading of the DMN in the noradrenergic enhancement circle of the LC, while the salience network is concomitant hyperactivated and increasingly upregulated for supporting the integration of novel information. Although results of DMN rs-fc show variable results comparing MCI and healthy controls, decrease of PCC activity seems to be the most prevailing pattern and fits well to our finding of LC-PCC reduction of fc (Eyler et al., 2019; Wang et al., 2012).

We could replicate that LC connectivity to the left parahippocampal gyrus is reduced in MCI patients, which was previously reported (Engels et al., 2020; Jacobs et al., 2015). The LC connectivity to parahippocampal gyrus is directly involved in memory functions (Berridge & Foote, 1991; Mather et al., 2016) and was found to be related to cognitive decline and beta-amyloid (Engels et al., 2020). Our result further supports those recent findings and validates the former results with our approach of extracting the LC BOLD signal from the individual anatomical location of the nucleus.

To further corroborate our pure fMRI results we assessed the relationship of LC resting state fc to MMSE scores. Importantly, the right LOC showed both a reduction in LC fc in MCI patients and a relationship between LC fc and MMSE scores. This connectivity of LC to right LOC can be attributed to the noradrenergic influence on the

temporoparietal junction (TPJ; for anatomical delineation as part of the LOC see Schurz et al., 2017). TPJ activity is suppressed during focussed attention, which supports ongoing task demands, and enhanced when new, unexpected stimuli enter the brain, accompanied by the EEG P300 wave (Aston-Jones & Cohen, 2005b; Knight et al., 1989; Verleger et al., 1994; Yamaguchi & Knight, 1992). The disturbances in LC to right TPJ connectivity fit to the idea of hyperactivated salience processing in MCI patients, may be a correlate to reduced LC phasic bursts (Aston-Jones & Cohen, 2005b; Braga et al., 2013; Corbetta et al., 2008; Janitzky, 2020; Vossel et al., 2014) and relevant for the known symptoms of behavioural flexibility decline in MCI patients (Guarino et al., 2020). Since we found a positive correlation between LC-TPJ rs-fc and MMSE scores, we speculate that LC-TPJ connectivity may be a connection that could serve as a marker for improvement of symptom severity in certain disease stages.

Then, we uncovered that the LC rs-fc to left parahippocampal gyrus differs between MCI and control groups in the relationship to MMSE score correlations, which further extends our result of reduced LC parahippocampal connectivity in MCI, as pointed out before.

Regarding salience network fc, MMSE score correlations differed between MCI and Control groups in the frontal pole, which was found to be less connected in the MCI group. In more detail, we found a negative correlation of the connectivity to that frontal area in high MMSE score patients. This means, that patients with higher MMSE scores will be able to decrease their pathological elevated salience network connectivity to frontal pole. On the other hand, we found that MCI patients lack on a relationship between MMSE scores to salience network connectivity to middle frontal brain including the paracingulate gyrus. Decreased salience network connectivity to superior and inferior frontal gyrus and to bilateral frontal pole was also found in trait anxiety (Geng et al., 2016) and panic disorder patients (Pannekoek et al., 2013), interpreted as lack of cognitive control. Elevated salience network connectivity to certain parts of the frontal brain by lack of correlation of central frontal brain connectivity to MMSE scores supports the idea of both disturbances regarding cognitive control in MCI patients, and a compensatory mechanism trying to balance this deficiency.

Summing up, the results of functional disturbances in MCI patients in comparison to an age-matched healthy control group and the relation to their MMSE scores come together in important brain regions for salience processing and emphasise how these brain structures are involved in the pathogenesis of early dementia.

On an electrophysiological level about LC function, neurodegenerative diseases were conceptualised as overactivation of LC tonic mode and decrease of LC phasic discharge (Janitzky, 2020), a model that would be in line with the rs functional disturbances we found here: we would expect elevated ACC-LC, LC-insula and salience network connectivity with elevated LC tonic mode (Aston-Jones & Cohen, 2005b) and a decrease of LC TPJ connectivity could be a correlate of decreased likelihood of phasic LC responses to novel information (Corbetta et al., 2008; Figure 2d, model). Janitzky (2020) pointed out how elevation of phasic LC response by vagal stimulation could

be a potential therapeutic option for MCI patients, which would be in line with a reconfiguration of LC-right TPJ connectivity (Corbetta et al., 2008). Essentially, since an overactivation of the LC tonic mode could be a negative predictor for disease progression, our results could provide a marker of the vulnerability of MCI patients for conversion to more severe dementia.

4.1 | Limitations

We did not find strong LC-ACC and LC-thalamic connectivity as previously described in our young healthy subject population (Liebe et al., 2020), which may be due to differences in rs alerting axis in elderly or may be more easily to uncover with ultra-high field strengths (7 T and above).

There is ongoing research about sub-specifying the origin of the hyperintense signal of neuromelanin in the MRI, which will aid better interpretability of our contrast ratio results in respect to clinical symptoms (Keren et al., 2015; Priovoulos et al., 2020).

The sensitivity of the MMSE score in the assessment of dementia is under debate (Creavin et al., 2016), but we evaluated our result by additionally analysing LC connectivity in respect to a summary score of all CERAD sub-scores (based on principal component analysis), further underpinning the importance of LC-ACC and LC-left insular connectivity in the functional pathogenesis of dementia (Text S1, Figures S3, S4, and Table S1).

Although longitudinal data collection is in progress, so far there is no follow-up data of our patient group in a stage when conversion from MCI to more severe forms of dementia can be expected. These data will inform, in which extend LC rs-fc can predict conversion to more severe disease. In this study and at this point, we provide stationary data about the network disturbances in our patients.

Although the connectivity differences between groups found here can inform about disturbances in MCI signal processing, some of the changes may be compensatory and help patients to maintain behavioural performance. Thus, task-based fMRI studies and longitudinal studies are needed to further investigate the relationship between MCI-related behavioural scores and the rs-fc changes found here, to underpin and further restrain the results with the aim to target those alterations of brain networks with new therapeutic strategies.

4.2 | Conclusions

By starting with localisation-based LC connectivity analysis followed by constrained hypotheses on brain networks, we could show that LC LOC connectivity, LC parahippocampal connectivity, LC left anterior insula connectivity and salience network to frontal brain connectivity are important pathways in the disturbances of MCI. The networks found affected here also showed a relationship to the widely used, clinical relevant MMSE score of dementia, which was strongly altered in our MCI patients compared with our healthy age-matched control group and related to impaired LC signal intensity, underpinning the

relevance of those networks in the functional pathogenesis of dementia. The attentional processing networks found disturbed in early dementia in this study and their theoretical implications could serve as targets for development of prevention strategies and therapeutics, and aid diagnostics and monitoring of treatment in dementia. Last, our study encourages the use of subject-specific masks to delineate the LC for fMRI measurements.

ACKNOWLEDGEMENTS

Funded by the Deutsche Forschungsgemeinschaft (DFG, German Research Foundation) - Projektnummer 41466077. Thomas Liebe is supported by the Deutsche Forschungsgemeinschaft (DFG, German Research Foundation) - 449879371. We would like to thank Friederike Mühler and Ilona Wiedenhoef for their help during data acquisition. Open Access funding enabled and organized by Projekt DEAL.

CONFLICT OF INTEREST

The authors declare that the research was conducted in the absence of any commercial or financial relationships that could be perceived as a real or apparent conflict of interest in the context of this publication.

DATA AVAILABILITY STATEMENT

The datasets generated during and/or analysed during the current study are available from the corresponding author on reasonable request.

ORCID

Notger Müller  <https://orcid.org/0000-0002-5483-6423>

REFERENCES

- Arevalo-Rodriguez, I., Smailagic, N., Figuls, M. R. I., Ciapponi, A., Sanchez-Perez, E., Giannakou, A., Pedraza, O. L., Cosp, X. B., & Cullum, S. (2015). Mini-mental state examination (MMSE) for the detection of Alzheimer's disease and other dementias in people with mild cognitive impairment (MCI). *Cochrane Database of Systematic Reviews*, 2015(3), CD010783. <https://doi.org/10.1002/14651858.CD010783>
- Aston-Jones, G., & Cohen, J. D. (2005a). Adaptive gain and the role of the locus coeruleus-norepinephrine system in optimal performance. *The Journal of Comparative Neurology*, 493(1), 99–110.
- Aston-Jones, G., & Cohen, J. D. (2005b). An integrative theory of locus coeruleus-norepinephrine function: Adaptive gain and optimal performance. *Annual Review of Neuroscience*, 28, 403–450.
- Baddeley, A., Cocchini, G., Della Sala, S., Logie, R. H., & Spinnler, H. (1999). Working memory and vigilance: Evidence from Normal aging and Alzheimer's disease. *Brain and Cognition*, 41(1), 87–108.
- Balthazar, M. L. F., de Campos, B. M., Franco, A. R., Damasceno, B. P., & Cendes, F. (2014). Whole cortical and default mode network mean functional connectivity as potential biomarkers for mild Alzheimer's disease. *Psychiatry Research: Neuroimaging*, 221(1), 37–42.
- Barnett, J. H., Lewis, L., Blackwell, A. D., & Taylor, M. (2014). Early intervention in Alzheimer's disease: A health economic study of the effects of diagnostic timing. *BMC Neurology*, 14(1), 101. <https://doi.org/10.1186/1471-2377-14-101>
- Berardi, A. M., Parasuraman, R., & Haxby, J. V. (2005). Sustained attention in mild Alzheimer's disease. *Developmental Neuropsychology*, 28(1), 507–537. https://doi.org/10.1207/s15326942dn2801_4
- Berridge, C., & Foote, S. (1991). Effects of locus coeruleus activation on electroencephalographic activity in neocortex and hippocampus. *The*

- Journal of Neuroscience*, 11(10), 3135–3145. <https://doi.org/10.1523/JNEUROSCI.11-10-03135.1991>
- Berridge, C. W., & Waterhouse, B. D. (2003). The locus coeruleus-noradrenergic system: Modulation of behavioral state and state-dependent cognitive processes. *Brain Research Reviews*, 42(1), 33–84.
- Betts, M. J., Cardenas-Blanco, A., Kanowski, M., Spottke, A., Teipel, S. J., Kilimann, I., Jessen, F., & Düzel, E. (2019). Locus coeruleus MRI contrast is reduced in Alzheimer's disease dementia and correlates with CSF A β levels. *Alzheimer's & Dementia: Diagnosis, Assessment & Disease Monitoring*, 11(1), 281–285. <https://doi.org/10.1016/j.dadm.2019.02.001>
- Bonthuis, D. J., Solodkin, A., & Van Hoesen, G. W. (2005). Pathology of the insular cortex in Alzheimer disease depends on cortical architecture. *Journal of Neuropathology and Experimental Neurology*, 64(10), 910–922. <https://doi.org/10.1097/01.jnen.0000182983.87106.d1>
- Bradford, A., Kunik, M. E., Schulz, P., Williams, S. P., & Singh, H. (2009). Missed and delayed diagnosis of dementia in primary care: Prevalence and contributing factors. *Alzheimer Disease & Associated Disorders*, 23(4), 306–314.
- Braga, R. M., Wilson, L. R., Sharp, D. J., Wise, R. J. S., & Leech, R. (2013). Separable networks for top-down attention to auditory non-spatial and visuospatial modalities. *NeuroImage*, 74, 77–86.
- Brandt, J., Aretouli, E., Neijstrom, E., Samek, J., Manning, K., Albert, M. S., & Bandeen-Roche, K. (2009). Selectivity of executive function deficits in mild cognitive impairment. *Neuropsychology*, 23(5), 607–618. <https://doi.org/10.1037/a0015851>
- Cao, Q., Tan, C. C., Xu, W., Hu, H., Cao, X. P., Dong, Q., Tan, L., & Yu, J. T. (2020). The prevalence of dementia: A systematic review and meta-analysis. *Journal of Alzheimer's Disease*, 73(3), 1157–1166. <https://doi.org/10.3233/JAD-191092>
- Cha, J., Jo, H. J., Kim, H. J., Seo, S. W., Kim, H. S., Yoon, U., Park, H., Na, D. L., & Lee, J. M. (2013). Functional alteration patterns of default mode networks: Comparisons of normal aging, amnesic mild cognitive impairment and Alzheimer's disease. *European Journal of Neuroscience*, 37(12), 1916–1924. <https://doi.org/10.1111/ejn.12177>
- Clewett, D. V., Lee, T. H., Greening, S., Ponzio, A., Margalit, E., & Mather, M. (2016). Neuromelanin marks the spot: Identifying a locus coeruleus biomarker of cognitive reserve in healthy aging. *Neurobiology of Aging*, 37, 117–126.
- Corbetta, M., Patel, G., & Shulman, G. L. (2008). The reorienting system of the human brain: From environment to theory of mind. *Neuron*, 58(3), 306–324.
- Costa, R. Q. M. D., Pompeu, J. E., de Viveiro, L. A. P., & Brucki, S. M. D. (2020). Spatial orientation tasks show moderate to high accuracy for the diagnosis of mild cognitive impairment: A systematic literature review. *Arquivos de Neuro-Psiquiatria*, 78(11), 713–723.
- Coughlan, G., Laczó, J., Hort, J., Minihane, A. M., & Hornberger, M. (2018). Spatial navigation deficits – Overlooked cognitive marker for preclinical Alzheimer disease? *Nature Reviews Neurology*, 14(8), 496–506.
- Creavin, S. T., Wisniewski, S., Noel-Storr, A. H., Trevelyan, C. M., Hampton, T., Rayment, D., Thom, V. M., Nash, K. J. E., Elhamoui, H., Milligan, R., Patel, A. S., Tsvos, D. V., Wing, T., Phillips, E., Kellman, S. M., Shackleton, H. L., Singleton, G. F., Neale, B. E., Watton, M. E., ... Cochrane Dementia and Cognitive Improvement Group. (2016). Mini-mental state examination (MMSE) for the detection of dementia in clinically unevaluated people aged 65 and over in community and primary care populations. *Cochrane Database of Systematic Reviews*, 2016(1), CD011145. <https://doi.org/10.1002/14651858.CD011145.pub2>
- Crous-Bou, M., Minguillón, C., Gramunt, N., & Molinuevo, J. L. (2017). Alzheimer's disease prevention: From risk factors to early intervention. *Alzheimer's Research & Therapy*, 9(1), 71. <https://doi.org/10.1186/s13195-017-0297-z>
- Dordevic, M., Müller-Fötti, A., Müller, P., Schmicker, M., Kaufmann, J., & Müller, N. G. (2017). Optimal cut-off value for locus Coeruleus-to-pons intensity ratio as clinical biomarker for Alzheimer's disease: A pilot study. *Journal of Alzheimer's Disease Reports*, 1(1), 159–167.
- Elman, J. A., Puckett, O. K., Beck, A., Fennema-Notestine, C., Cross, L. K., Dale, A. M., Eglit, G. M. L., Eyer, L. T., Gillespie, N. A., Granholm, E. L., Gustavson, D. E., Hagler, D. J., Jr., Hatton, S. N., Hauger, R., Jak, A. J., Logue, M. W., McEvoy, L. K., McKenzie, R. E., Neale, M. C., ... Kremen, W. S. (2021). MRI-assessed locus coeruleus integrity is heritable and associated with multiple cognitive domains, mild cognitive impairment, and daytime dysfunction. *Alzheimer's & Dementia*, 17(6), 1017–1025. <https://doi.org/10.1002/alz.12261>
- Engels, N., Prokopiou, P. C., Uquillas, F.d., Scott, M. R., Schultz, A. P., Papp, K. V., Farrell, M. E., Rentz, D. M., Sperling, R. A., Johnson, K. A., & Jacobs, H. I. L. (2020). Hypoconnectivity between locus coeruleus and medial temporal lobe during novelty predicts accelerated A β -related cognitive decline: The locus coeruleus: Nexus of behavioral and cognitive problems in dementia. *Alzheimer's & Dementia*, 16(S2), e041323. <https://doi.org/10.1002/alz.041323>
- Eyer, L. T., Elman, J. A., Hatton, S. N., Gough, S., Mischel, A. K., Hagler, D. J., Franz, C. E., Docherty, A., Fennema-Notestine, C., Gillespie, N., Gustavson, D., Lyons, M. J., Neale, M. C., Panizzon, M. S., Dale, A. M., & Kremen, W. S. (2019). Resting state abnormalities of the default mode network in mild cognitive impairment: A systematic review and meta-analysis. *Journal of Alzheimer's Disease*, 70(1), 107–120. <https://doi.org/10.3233/JAD-180847>
- Farb, N. A. S., Segal, Z. V., & Anderson, A. K. (2013). Attentional modulation of primary interoceptive and Exteroceptive cortices. *Cerebral Cortex*, 23(1), 114–126. <https://doi.org/10.1093/cercor/bhr385>
- Faust, M. E., & Balota, D. A. (1997). Inhibition of return and visuospatial attention in healthy older adults and individuals with dementia of the Alzheimer type. *Neuropsychology*, 11(1), 13–29. <https://doi.org/10.1037/0894-4105.11.1.13>
- Fischl, B. (2012). FreeSurfer. *NeuroImage*, 62(2), 774–781.
- Geng, H., Li, X., Chen, J., Li, X., & Gu, R. (2016). Decreased intra- and inter-salience network functional connectivity is related to trait anxiety in adolescents. *Frontiers in Behavioral Neuroscience*, 9, 350. <https://doi.org/10.3389/fnbeh.2015.00350/abstract>
- German, D. C., Manaye, K. F., White, C. L., 3rd, Woodward, D. J., McIntire, D. D., Smith, W. K., Kalaria, R. N., & Mann, D. M. (1992). Disease-specific patterns of locus coeruleus cell loss. *Annals of Neurology*, 32(5), 667–676. <https://doi.org/10.1002/ana.410320510>
- Glasser, M. F., Coalson, T. S., Robinson, E. C., Hacker, C. D., Harwell, J., Yacoub, E., Ugurbil, K., Andersson, J., Beckmann, C. F., Jenkinson, M., Smith, S. M., & van Essen, D. C. (2016). A multi-modal parcellation of human cerebral cortex. *Nature*, 536(7615), 171–178.
- Guarino, A., Forte, G., Giovannoli, J., & Casagrande, M. (2020). Executive functions in the elderly with mild cognitive impairment: A systematic review on motor and cognitive inhibition, conflict control and cognitive flexibility. *Aging & Mental Health*, 24(7), 1028–1045. <https://doi.org/10.1080/13607863.2019.1584785>
- Jacobs, H. I. L., Müller-Ehrenberg, L., Priovoulos, N., & Roebroeck, A. (2018). Curvilinear locus coeruleus functional connectivity trajectories over the adult lifespan: A 7T MRI study. *Neurobiology of Aging*, 69, 167–176.
- Jacobs, H. I. L., Wiese, S., van de Ven, V., Gronenschild, E. H., Verhey, F. R. J., & Matthews, P. M. (2015). Relevance of parahippocampal-locus coeruleus connectivity to memory in early dementia. *Neurobiology of Aging*, 36(2), 618–626.
- Janitzky, K. (2020). Impaired phasic discharge of locus Coeruleus neurons based on persistent high tonic discharge—A new hypothesis with potential implications for neurodegenerative diseases. *Frontiers in Neurology*, 11, 371. <https://doi.org/10.3389/fneur.2020.00371/full>
- Keren, N. I., Lozar, C. T., Harris, K. C., Morgan, P. S., & Eckert, M. A. (2009). In vivo mapping of the human locus coeruleus. *NeuroImage*, 47(4), 1261–1267.

- Keren, N. I., Taheri, S., Vazey, E. M., Morgan, P. S., Granholm, A. C. E., Aston-Jones, G. S., & Eckert, M. A. (2015). Histologic validation of locus coeruleus MRI contrast in post-mortem tissue. *NeuroImage*, 113, 235–245.
- Knight, R. T., Scabini, D., Woods, D. L., & Clayworth, C. C. (1989). Contributions of temporal-parietal junction to the human auditory P3. *Brain Research*, 502(1), 109–116.
- Lee, T.-H., Kim, S. H., Katz, B., & Mather, M. (2020). The decline in intrinsic connectivity between the salience network and locus Coeruleus in older adults: Implications for distractibility. *Frontiers in Aging Neuroscience*, 12, 2. <https://doi.org/10.3389/fnagi.2020.00002/full>
- Liao, Z.-L., Tan, Y. F., Qiu, Y. J., Zhu, J. P., Chen, Y., Lin, S. S., Wu, M. H., Mao, Y. P., Hu, J. J., Ding, Z. X., & Yu, E. Y. (2018). Interhemispheric functional connectivity for Alzheimer's disease and amnesic mild cognitive impairment based on the triple network model. *Journal of Zhejiang University-Science B*, 19(12), 924–934. <https://doi.org/10.1631/jzus.B1800381>
- Liebe, T., Kaufmann, J., Li, M., Skalej, M., Wagner, G., & Walter, M. (2020). In vivo anatomical mapping of human locus coeruleus functional connectivity at 3 T MRI. *Human Brain Mapping*, 41, 2136–2151. <https://doi.org/10.1002/hbm.24935>
- Liebe, T., Li, M., Colic, L., Munk, M. H. J., Sweeney-Reed, C. M., Woelfer, M., Kretschmar, M. A., Steiner, J., von Düring, F., Behnisch, G., Schott, B. H., & Walter, M. (2018). Ketamine influences the locus coeruleus norepinephrine network, with a dependency on norepinephrine transporter genotype – A placebo controlled fMRI study. *NeuroImage: Clinical*, 20, 715–723.
- Lin, F., Ren, P., Lo, R. Y., Chapman, B. P., Jacobs, A., Baran, T. M., Porsteinsson, A. P., Foxe, J. J., & Alzheimer's Disease Neuroimaging Initiative. (2016). Insula and inferior frontal gyrus' activities protect memory performance against Alzheimer's disease pathology in old age. *Journal of Alzheimer's Disease*, 55(2), 669–678. <https://doi.org/10.3233/JAD-160715>
- Liu, K. Y., Kievit, R. A., Tsvetanov, K. A., Betts, M. J., Düzel, E., Rowe, J. B., Cam-CAN, Howard, R., & Hämmerer, D. (2020). Noradrenergic-dependent functions are associated with age-related locus coeruleus signal intensity differences. *Nature Communications*, 11(1), 1712.
- Lorking, N., Murray, A. D., & O'Brien, J. T. (2021). The use of positron emission tomography/magnetic resonance imaging in dementia: A literature review. *International Journal of Geriatric Psychiatry*, 36(10), 1501–1513. <https://doi.org/10.1002/gps.5586>
- Lu, L., Li, F., Chen, H., Wang, P., Zhang, H., Chen, Y. C., & Yin, X. (2020). Functional connectivity dysfunction of insular subdivisions in cognitive impairment after acute mild traumatic brain injury. *Brain Imaging and Behavior*, 14(3), 941–948. <https://doi.org/10.1007/s11682-020-00288-5>
- Markesbery, W. R. (2010). Neuropathologic alterations in mild cognitive impairment: A review. *Journal of Alzheimer's Disease*, 19(1), 221–228. <https://doi.org/10.3233/JAD-2010-1220>
- Mather, M., Clewett, D., Sakaki, M., & Harley, C. W. (2016). Norepinephrine ignites local hotspots of neuronal excitation: How arousal amplifies selectivity in perception and memory. *Behavioral and Brain Sciences*, 39, e200.
- McCarthy, J., Collins, D. L., & Ducharme, S. (2018). Morphometric MRI as a diagnostic biomarker of frontotemporal dementia: A systematic review to determine clinical applicability. *NeuroImage: Clinical*, 20, 685–696. <https://doi.org/10.1016/j.nicl.2018.05.010>
- McKhann, G., Drachman, D., Folstein, M., Katzman, R., Price, D., & Stadlan, E. M. (1984). Clinical diagnosis of Alzheimer's disease: Report of the NINCDS-ADRDA work group under the auspices of Department of Health and Human Services Task Force on Alzheimer's disease. *Neurology*, 34(7), 939–944. <https://doi.org/10.1212/WNL.34.7.939>
- Mesulam, M. M., & Mufson, E. J. (1982). Insula of the old world monkey. III: Efferent cortical output and comments on function. *The Journal of Comparative Neurology*, 212(1), 38–52. <https://doi.org/10.1002/cne.902120104>
- Moon, Y., Moon, W. J., Kim, H., & Han, S. H. (2014). Regional atrophy of the insular cortex is associated with neuropsychiatric symptoms in Alzheimer's disease patients. *European Neurology*, 71(5–6), 223–229.
- Murphy, P. R., O'Connell, R. G., O'Sullivan, M., Robertson, I. H., & Balsters, J. H. (2014). Pupil diameter covaries with BOLD activity in human locus coeruleus. *Human Brain Mapping*, 35(8), 4140–4154.
- Olivieri, P., Lagarde, J., Lehericy, S., Valabrègue, R., Michel, A., Macé, P., Caillé, F., Gervais, P., Bottlaender, M., & Sarazin, M. (2019). Early alteration of the locus coeruleus in phenotypic variants of Alzheimer's disease. *Annals of Clinical and Translational Neurology*, 6(7), 1345–1351. <https://doi.org/10.1002/acn3.50818>
- Pannekoek, J. N., Veer, I. M., van Tol, M. J., van der Werff, S. J. A., Demenescu, L. R., Aleman, A., Veltman, D. J., Zitman, F. G., Rombouts, S. A. R. B., & van der Wee, N. J. A. (2013). Aberrant limbic and salience network resting-state functional connectivity in panic disorder without comorbidity. *Journal of Affective Disorders*, 145(1), 29–35.
- Périn, B., Godefroy, O., Fall, S., & de Marco, G. (2010). Alertness in young healthy subjects: An fMRI study of brain region interactivity enhanced by a warning signal. *Brain and Cognition*, 72(2), 271–281.
- Petersen, S. E., & Posner, M. I. (2012). The attention system of the human brain: 20 years after. *Annual Review of Neuroscience*, 35, 73–89.
- Philippi, N., Noblet, V., Hamdaoui, M., Soulier, D., Botzung, A., Ehrhard, E., Cretin, B., Blanc, F., & AlphaLewyMA study group. (2020). The insula, a grey matter of tastes: A volumetric MRI study in dementia with Lewy bodies. *Alzheimer's Research & Therapy*, 12(1), 79. <https://doi.org/10.1186/s13195-020-00645-y>
- Posner, M. I. (2012). Imaging attention networks. *NeuroImage*, 61(2), 450–456.
- Prince, M., Bryce, R., Albanese, E., Wimo, A., Ribeiro, W., & Ferri, C. P. (2013). The global prevalence of dementia: A systematic review and metaanalysis. *Alzheimer's & Dementia*, 9(1), 63. <https://doi.org/10.1016/j.jalz.2012.11.007>
- Priovoulos, N., van Boxel, S. C. J., Jacobs, H. I. L., Poser, B. A., Uludag, K., Verhey, F. R. J., & Ivanov, D. (2020). Unraveling the contributions to the neuromelanin-MRI contrast. *Brain Structure and Function*, 225(9), 2757–2774. <https://doi.org/10.1007/s00429-020-02153-z>
- Redel, P., Bublak, P., Sorg, C., Kurz, A., Förstl, H., Müller, H. J., Schneider, W. X., Perneczky, R., & Finke, K. (2012). Deficits of spatial and task-related attentional selection in mild cognitive impairment and Alzheimer's disease. *Neurobiology of Aging*, 33(1), 195.e27–195.e42.
- Reuter, M., Schmansky, N. J., Rosas, H. D., & Fischl, B. (2012). Within-subject template estimation for unbiased longitudinal image analysis. *NeuroImage*, 61(4), 1402–1418.
- Robinson, L., Tang, E., & Taylor, J. P. (2015). Dementia: Timely diagnosis and early intervention. *BMJ*, 350, h3029. <https://doi.org/10.1136/bmj.h3029>
- Samuels, E., & Szabadi, E. (2008). Functional neuroanatomy of the noradrenergic locus Coeruleus: Its roles in the regulation of arousal and autonomic function part II: Physiological and pharmacological manipulations and pathological alterations of locus Coeruleus activity in humans. *Current Neuropharmacology*, 6(3), 254–285.
- Sanders, C., Low, C., & Schmitter-Edgecombe, M. (2014). Assessment of planning abilities in individuals with mild cognitive impairment using an open-ended problem-solving task. *Journal of Clinical and Experimental Neuropsychology*, 36(10), 1084–1097. <https://doi.org/10.1080/13803395.2014.983462>
- Saunders, N. L. J., & Summers, M. J. (2011). Longitudinal deficits to attention, executive, and working memory in subtypes of mild cognitive impairment. *Neuropsychology*, 25(2), 237–248. <https://doi.org/10.1037/a0021134>
- Schultz, A. P., Chhatwal, J. P., Hedden, T., Mormino, E. C., Hanseeuw, B. J., Sepulcre, J., Huijbers, W., LaPoint, M., Buckley, R. F., Johnson, K. A., & Sperling, R. A. (2017). Phases of Hyperconnectivity and Hypoconnectivity in the default mode and salience networks track with amyloid and tau in clinically Normal individuals. *The Journal of Neuroscience*,

- 37(16), 4323–4331. <https://doi.org/10.1523/JNEUROSCI.3263-16.2017>
- Schurz, M., Tholen, M. G., Perner, J., Mars, R. B., & Sallet, J. (2017). Specifying the brain anatomy underlying temporo-parietal junction activations for theory of mind: A review using probabilistic atlases from different imaging modalities: Brain anatomy underlying Temporo-parietal junction. *Human Brain Mapping*, 38(9), 4788–4805. <https://doi.org/10.1002/hbm.23675>
- Seeley, W. W. (2019). The salience network: A neural system for perceiving and responding to homeostatic demands. *The Journal of Neuroscience*, 39(50), 9878–9882. <https://doi.org/10.1523/JNEUROSCI.1138-17.2019>
- Seth, A. K. (2013). Interoceptive inference, emotion, and the embodied self. *Trends in Cognitive Sciences*, 17(11), 565–573.
- Seth, A. K., Suzuki, K., & Critchley, H. D. (2012). An interoceptive predictive coding model of conscious presence. *Frontiers in Psychology*, 2, 395. <https://doi.org/10.3389/fpsyg.2011.00395/abstract>
- Takahashi, J., Shibata, T., Sasaki, M., Kudo, M., Yanezawa, H., Obara, S., Kudo, K., Ito, K., Yamashita, F., & Terayama, Y. (2015). Detection of changes in the locus coeruleus in patients with mild cognitive impairment and Alzheimer's disease: High-resolution fast spin-echo T1-weighted imaging. *Geriatrics & Gerontology International*, 15(3), 334–340. <https://doi.org/10.1111/ggi.12280>
- Tomlinson, B. E., Irving, D., & Blessed, G. (1981). Cell loss in the locus coeruleus in senile dementia of Alzheimer type. *Journal of the Neurological Sciences*, 49(3), 419–428.
- Tournier, J.-D., Smith, R., Raffelt, D., Tabbara, R., Dhollander, T., Pietsch, M., Christiaens, D., Jeurissen, B., Yeh, C. H., & Connelly, A. (2019). MRtrix3: A fast, flexible and open software framework for medical image processing and visualisation. *NeuroImage*, 202, 116137.
- Tsoi, K. K. F., Chan, J. Y. C., Hirai, H. W., Wong, S. Y. S., & Kwok, T. C. Y. (2015). Cognitive tests to detect dementia: A systematic review and meta-analysis. *JAMA: Internal Medicine*, 175(9), 1450–1458. <https://doi.org/10.1001/jamainternmed.2015.2152>
- Tzourio-Mazoyer, N., Landeau, B., Papathanassiou, D., Crivello, F., Etard, O., Delcroix, N., Mazoyer, B., & Joliot, M. (2002). Automated anatomical labeling of activations in SPM using a macroscopic anatomical Parcellation of the MNI MRI single-subject brain. *NeuroImage*, 15(1), 273–289.
- Verleger, R., Heide, W., Butt, C., & Kömpf, D. (1994). Reduction of P3b in patients with temporo-parietal lesions. *Cognitive Brain Research*, 2(2), 103–116.
- Vossel, S., Geng, J. J., & Fink, G. R. (2014). Dorsal and ventral attention systems: Distinct neural circuits but collaborative roles. *The Neuroscientist*, 20(2), 150–159. <https://doi.org/10.1177/1073858413494269>
- Wagner, G., Krause-Utz, A., de la Cruz, F., Schumann, A., Schmahl, C., & Bär, K. J. (2018). Resting-state functional connectivity of neurotransmitter producing sites in female patients with borderline personality disorder. *Progress in Neuro-Psychopharmacology & Biological Psychiatry*, 83, 118–126.
- Wang, R. W. Y., Chang, W. L., Chuang, S. W., & Liu, I. N. (2019). Posterior cingulate cortex can be a regulatory modulator of the default mode network in task-negative state. *Scientific Reports*, 9(1), 7565.
- Wang, S., Sun, H., Hu, G., Xue, C., Qi, W., Rao, J., Zhang, F., Zhang, X., & Chen, J. (2021). Altered insular subregional connectivity associated with cognitions for distinguishing the Spectrum of pre-clinical Alzheimer's disease. *Frontiers in Aging Neuroscience*, 13, 597455. <https://doi.org/10.3389/fnagi.2021.597455/full>
- Wang, X., Wu, Q., Egan, L., Gu, X., Liu, P., Gu, H., Yang, Y., Luo, J., Wu, Y., Gao, Z., & Fan, J. (2019). Anterior insular cortex plays a critical role in interoceptive attention. *eLife*, 8, e42265.
- Wang, Z., Liang, P., Jia, X., Jin, G., Song, H., Han, Y., Lu, J., & Li, K. (2012). The baseline and longitudinal changes of PCC connectivity in mild cognitive impairment: A combined structure and resting-state fMRI study. *PLoS One*, 7(5), e36838. <https://doi.org/10.1371/journal.pone.0036838>
- Waninger, S., Berka, C., Meghdadi, A., Karic, M. S., Stevens, K., Agüero, C., Sitnikova, T., Salat, D. H., & Verma, A. (2018). Event-related potentials during sustained attention and memory tasks: Utility as biomarkers for mild cognitive impairment. *Alzheimer's & Dementia: Diagnosis, Assessment & Disease Monitoring*, 10(1), 452–460. <https://doi.org/10.1016/j.dadm.2018.05.007>
- Whitfield-Gabrieli, S., & Nieto-Castanon, A. (2012). Conn: A functional connectivity toolbox for correlated and anticorrelated brain networks. *Brain Connectivity*, 2(3), 125–141.
- Witzel, C., Olkkonen, M., & Gegenfurtner, K. R. (2018). A Bayesian model of the memory colour effect. *Perception*, 9(3), 204166951877171. <https://doi.org/10.1177/2041669518771715>
- Xie, C., Bai, F., Yu, H., Shi, Y., Yuan, Y., Chen, G., Li, W., Chen, G., Zhang, Z., & Li, S. J. (2012). Abnormal insula functional network is associated with episodic memory decline in amnesic mild cognitive impairment. *NeuroImage*, 63(1), 320–327.
- Yamaguchi, S., & Knight, R. T. (1992). Effects of temporal-parietal lesions on the somatosensory P3 to lower limb stimulation. *Electroencephalography and Clinical Neurophysiology/Evoked Potentials Section*, 84(2), 139–148.
- Yokoi, T., Watanabe, H., Yamaguchi, H., Bagarinao, E., Masuda, M., Imai, K., Ogura, A., Ohdake, R., Kawabata, K., Hara, K., Riku, Y., Ishigaki, S., Katsuno, M., Miyao, S., Kato, K., Naganawa, S., Harada, R., Okamura, N., Yanai, K., ... Sobue, G. (2018). Involvement of the Precuneus/posterior cingulate cortex is significant for the development of Alzheimer's disease: A PET (THK5351, PiB) and resting fMRI study. *Frontiers in Aging Neuroscience*, 10, 304. <https://doi.org/10.3389/fnagi.2018.00304/full>
- Zhang, S., Hu, S., Chao, H. H., & Li, C.-S. R. (2016). Resting-state functional connectivity of the locus Coeruleus in humans: In comparison with the ventral tegmental area/substantia Nigra pars compacta and the effects of age. *Cerebral Cortex (New York, N.Y.: 1991)*, 26(8), 3413–3427.
- Zheng, W., Cui, B., Han, Y., Song, H., Li, K., He, Y., & Wang, Z. (2019). Disrupted regional cerebral blood flow, functional activity and connectivity in Alzheimer's disease: A combined ASL perfusion and resting state fMRI study. *Frontiers in Neuroscience*, 13, 738. <https://doi.org/10.3389/fnins.2019.00738/full>
- Zhou, J., Greicius, M. D., Gennatas, E. D., Growdon, M. E., Jang, J. Y., Rabinovici, G. D., Kramer, J. H., Weiner, M., Miller, B. L., & Seeley, W. W. (2010). Divergent network connectivity changes in behavioural variant frontotemporal dementia and Alzheimer's disease. *Brain*, 133(5), 1352–1367. <https://doi.org/10.1093/brain/awq075>

SUPPORTING INFORMATION

Additional supporting information can be found online in the Supporting Information section at the end of this article.

How to cite this article: Liebe, T., Dordevic, M., Kaufmann, J., Avetisyan, A., Skalej, M., & Müller, N. (2022). Investigation of the functional pathogenesis of mild cognitive impairment by localisation-based locus coeruleus resting-state fMRI. *Human Brain Mapping*, 43(18), 5630–5642. <https://doi.org/10.1002/hbm.26039>